

## Depth migration Green's functions derived from VSP

Robert J. Ferguson

### ABSTRACT

Green's functions are obtained for depth migration in heterogeneous media through estimation of subsurface scattering-potential  $V$ . Multiple vertical-seismic profiles (VSPs) are used to compute  $V$ , and elastic variation and density variation estimated independently are used to perturb  $V$  to represent all surface / subsurface scattering potentials. Then,  $V$  for all points in the image space are converted to Green's functions for use in depth imaging.

In the absence of prior knowledge of elastic variation and density variation, perturbation of  $V$  is computed for common-offset, common-azimuth gathers under the assumption of smooth variation in velocity where density is constant. These assumptions are consistent with conventional moveout velocity, so perturbation of  $V$  from moveout analysis is developed.

### INTRODUCTION

Seismic images are 3-dimensional grids where seismic reflection strength (reflectivity) is mapped onto each grid node. The value of reflectivity at a grid node represents the lithologic contrast local to that node. Central to this mapping are numerical Green's functions\* that cause wave propagation from source grid-points to reflection grid-points. Green's functions are normally calculated using a velocity model that is inferred from analysis of recorded reflections. Many assumptions are made using this approach and the most important assumption is scalar wave-propagation. This assumption simplifies calculation, but it excludes a large class of non-Fermat waves like multiples and multi-path arrivals, and other modes that are recorded. Significant effort, therefore, is spent in approximation to wave propagation to adapt conventional Green's function based imaging to more and more complex geology.

Recently, there is growing interest in direct Green's function estimation to reduce dependence on model building to capture significantly more of the propagating wavefields. For example, in Brandesberg-Dahl et al. (2007), vertical-seismic profile (VSP) Green's functions are used to migrate surface data. Central to this method is the use of a single VSP, plus the assumption that the medium is homogeneous laterally. A Kirchhoff integral is then used to compute the image away from the VSP. Such methods rely on in-situ measurements in that the recorded wavefield in the subsurface is the Green's function associated with the source. The data/Green's function is then used as the imaging Green's function that maps reflectivity to image grid-locations local to the in-situ receiver.

For elastic media, Fishmann (2004) simulates wave-propagation analytically through a Fourier-integral operator. This approach is based on foreknowledge of the heterogeneity and anisotropy of the geology of interest. Rather than compute a two-way Green's

---

\*In this paper, my usage of *Green's* rather than *Green* follows the usage of Morse and Feshbach (1953).

function for the Fourier-integral operator, however, I see a natural relationship between Green's function estimation from recorded wavefields and simulation of wave propagation by Fourier-integral operator.

Because in-situ measurements are rarely distributed evenly within the image grid, in fact they are usually localized to well locations in the form of vertical seismic profiles (VSPs), the direct Green's function methods suffer decreased accuracy with distance from in-situ measurements. Inaccuracy becomes even more serious in heterogeneous/anisotropic settings. Seismic velocity analysis is routine, however, and because the resulting velocity model traverses the entire range of the imaging grid, it is natural to adapt scattering theory such that measured Green's functions may be extrapolated further away from the in-situ locations with greater accuracy.

Direct perturbation of measured Green's functions based on the velocity model is, of course, possible, but for mathematical tractability, direct perturbation would be based on the approximate, analytic Green's functions of conventional imaging. This approach, therefore, would impose the same limited range of propagating modes that the conventional approach suffers from. Instead, to model full-wave behaviour, I propose to estimate scattering potential  $V$  from in-situ measurements and then, with out loss of generality, deduce the required Green's functions. Then, for points far from the in-Situ locations, perturbation of the known Green's functions occurs as a result of perturbation of the scattering potential, and no assumption about propagating mode is required.

Because, however, prior knowledge of elasticity and density is usually sparse or unavailable, a constant-density assumption is invoked, and an approximate perturbation approached is presented. Then, because S-wave velocity is rarely obtained on a wide scale, the ratio of P- and S-wave velocity is assumed constant, and a further approximation to the perturbation approach is presented based on P-wave velocity alone.

## Theory

For point source  $\delta(x_s - x)$ , where coordinates  $x \in \mathfrak{R}^3$  are associated with points of observation, and  $x_s \in \mathfrak{R}^3$  are source points, Green's function  $G(x|x_s)$  (Morse and Feshbach (1953) p.g. 493) converts  $\delta$  into observed, monochromatic wavefield  $\psi(x)$  according to

$$\psi(x) = [G(x|x_s) S \delta(x_s - x)](x), \quad (1)$$

where  $S$  is a monochromatic scalar associated with the source. Given a monochromatic wavefield, from a VSP for example, and given  $S$  for the source,  $G$  may be deduced following Brandesberg-Dahl et al. (2007).  $G$ , then, can be used to model  $\psi(x)$  exactly. For wavefield  $\psi(y)$  at observation point  $y \neq x$ ,  $G(y|x_s)$  may be deduced also. Given two reference  $G$ s, then, we depart the method of Brandesberg-Dahl et al. (2007) and turn to the Lippmann-Schwinger equation

$$G = G_r + G_r V G, \quad (2)$$

where  $G$  is desired (found on both sides of equation 2),  $G_r$  is known (conventionally, an approximate operator (Clayton and Stolt, 1981)), and  $V$  is scattering-potential according

to

$$V = \omega^2 \left( \frac{1}{\kappa} - \frac{1}{\kappa_r} \right) + \nabla \cdot \left( \frac{1}{\rho} - \frac{1}{\rho_r} \right) \nabla, \quad (3)$$

where  $\nabla$  and  $\nabla \cdot$  are the gradient operator and divergence operators of 3-space respectively (Clayton and Stolt, 1981). Variables  $\kappa_r$  and  $\rho_r$  are bulk-modulus and density at the reference point, and  $\omega$  is the frequency of the monochromatic source. Variables  $\kappa$  and  $\rho$  correspond to bulk modulus and density at the point of desired  $G$ . Rather than estimate  $G$ , as is the conventional use of Lippmann-Schwinger (Clayton and Stolt, 1981), and given  $G(x|x_s)$  and  $G(y|x_s)$ , then according to equation 2, we may deduce instead scattering-potential  $V$  for the region between  $x$  and  $y$ . Modify equation 2 so that

$$G(x|x_s) = G(y|x_s) + G(y|x_s) V(x, y|x_s) G(x|x_s), \quad (4)$$

where  $G(x|x_s)$  is associated with location  $x$  due to a source at  $x_s$ ,  $G(y|x_s)$  is associated, similarly, with location  $y \in \mathfrak{R}^3$  and source  $x_s$ , and  $V$  is the scattering potential between  $x$  and  $y$  associated with source  $x_s$ . Solution  $\tilde{V} \approx V$  for equation 4 is the scattering potential of the region between  $x$  and  $y$  for a source that is an appropriate distance from  $x_s$ .

For any desired  $G(z|x_s)$ , where  $x \leq z \leq y, z \in \mathfrak{R}^3$ , we employ  $\tilde{V}$  according to

$$G_x(z|x_s) = G(x|x_s) + G(x|x_s) \tilde{V}(x, y|x_s) G(z|x_s)_x, \quad (5)$$

where subscript  $x$   $G_x(z|x_s)$  based on  $G(x|x_s)$ . Alternatively, based  $G(y|x_s)$ , we have

$$G_y(z|x_s) = G(y|x_s) + G(y|x_s) \tilde{V}(x, y|x_s) G_y(y|x_s). \quad (6)$$

Of course, combinations of equation 6 can be contemplated to help improve  $G(z|x_s)$ . A weighted average of equations (5) and (6), for example, is appropriate according to

$$G_{xy}(z|x_s) = \varepsilon(x|y) [\varphi(x|y) G_x(z|x_s) + G_y(z|x_s)], \quad (7)$$

where  $\varphi$  is a weight function that depends on where  $z$  lies relative to  $x$  and  $y$ , and  $\varepsilon$  is a function that normalizes the result.

Based on equations 5, 6, or 7,  $G_x(z|x_s)$ , from equation 5 for example, is available to model wavefield  $\psi(z)$  for source point  $S \delta(x_s - z)$  according to

$$\psi(z) = [G_x(z|x_s) S \delta(x_s - x)](z). \quad (8)$$

Modelling is demonstrated schematically in Figures 1a, b, c, and d. Here, a seismic experiment is designed such that a source (black dot labelled  $x_s$  Figure 1a) and two VSP locations (red circles labelled  $x$  and  $y$  Figure 1a) are selected over a region of interest. Figure 1b shows the survey geometry in depth (the VSP receivers are red circles connected with a black line). In Figures 1a and b, the green circles represent locations of desired  $G$ s (locations  $z$  and  $z'$ ), and the green dot represents a virtual source associated with receiver location  $z$ . The source at  $x_s$  is detonated, and wavefields are recorded at VSP locations  $x$  and  $y$  as shown in Figure 1c.

The VSP wavefields, interpreted as  $G(x|x_s)$  and  $G(y|x_s)$ , are input to equation 4, and scattering potential  $\tilde{V}(x|y)$  is computed. Scattering potential  $\tilde{V}(x|y)$  represents the

scattering potential between  $x$  and  $y$  for a source at  $x_s$ . For point  $z$  intermediate to  $x$  and  $y$ , compute  $G_x(z|x_{z,s})$  for virtual source location  $x_{z,s}$  using wavefield  $G(x|x_s) = \psi(x, x_s)$  and equation 5 (or equation 6, or equation 7). The computed  $G$  for  $z$  is shown schematically in Figure 1 (right side). Location  $z$  is inline with  $x_s$ ,  $x$  and  $y$ , and distances  $\overline{x_s x} = \overline{x_{z,s} z}$ , so it is natural to assume that  $\tilde{V}$  will map  $G(x|x_s) \rightarrow G_x(z|x_s)$  according to equation 4.

For location  $z'$ , however, though distances  $\overline{x_s x} = \overline{x_s z'}$ , azimuths  $\phi_{x,x_s} \neq \phi_{z',x_s}$ , and, if the geology is variable and anisotropic,  $\tilde{V}$  is a very approximate estimate of the true scattering potential.  $G_x(z'|x_s)$  (Figure 1d, left side), in this basic form, is inaccurate for geology that is heterogeneous and anisotropic, and wavefield  $\psi_x(z)$  computed according to equation 8 will be, likewise, erroneous for offline location  $z'$ .

Because seismic-velocity analysis is routine, velocity variation in space is available to guide how  $G$  for a region is modified to suit a different region, and it is natural to do this through modification of scattering potential  $\tilde{V}$ .

### Perturbed $V$

Suppose that, given prior knowledge of geologic variation between  $x$  and  $z'$ , we can modify scattering potential  $\tilde{V}$  so that it is suitable for location  $z'$  according to

$$\tilde{V}(z', x|x_s) = \tilde{V}(x, y|x_s) + \Delta V \quad (9)$$

with perturbation term  $\Delta V$  given as a series evaluated at  $x$

$$\Delta V = \sum_{j=1}^{\infty} \frac{\Delta x^j}{j!} \left. \frac{\partial^j V}{\partial x^j} \right|_x, \quad (10)$$

and where  $\Delta x$  is the distance between locations  $x$  and  $z'$ . Spatial derivatives of  $V$ , of course, will result in complicated functions of the spatial derivatives of  $\kappa$  and  $\rho$ .

Given  $\Delta V$ , then,  $G$  for location  $z'$  is now an improved estimate according to (from equation 5)

$$G_x(z'|x_s) \approx G(x|x_s) + G(x|x_s) \left[ \tilde{V}(x, y|x_s) + \Delta V \right] G_x(z|x_s). \quad (11)$$

With good knowledge of  $\kappa$  and  $\rho$  variation, calculation of  $\Delta V$  directly is possible as it is, though and a number of difficulties present themselves. For example,  $V$  (equation 3) has  $\nabla$  operators in the second term that might be difficult to implement numerically. Also, both terms are rather awkward functions of bulk modulus  $\kappa$  and density  $\rho$ . To simplify, for clarity at least, assume constant  $\rho$ , and assume that the ratio of body-wave velocities ( $\gamma = \alpha/\beta$ ) is constant also to get (equation A-4 Appendix A)

$$\Delta V \approx (1 + \gamma^{-1}) \sum_{j=1}^{\infty} \frac{\Delta \alpha^j}{j!} \left. \frac{\partial^j V}{\partial \alpha^j} \right|_x, \quad (12)$$

where  $\Delta \alpha$  is the difference between  $\alpha_x$  and  $\alpha_{z'}$ .

The prescription for  $\Delta V$  simplifies even further for acoustic media ( $\alpha = \sqrt{k\rho}$ ) when  $\alpha$  varies smoothly. For the acoustic case we have from Appendix A

$$\Delta V \approx \left[ V + \left( \frac{\omega}{\alpha_z} \right)^2 \frac{1}{\rho} \right] \sum_{j=1}^N (-1)^{(j+1)} (j+1) \left( \frac{\Delta\alpha}{\alpha_x} \right)^j \quad (13)$$

where  $N \sim 100$  ensures accuracy for reasonable cost.

## DISCUSSION

The use of the approximations given in equations 13 and 12 to simplify and speed calculation of perturbed scattering-potential  $V + \Delta V$  may or may not be necessary where considerable resources are available for computation, and where P- and S-velocity variation plus density variation is well understood. Where resources and information are limited, then equations 13 and 12 may find considerable utility.

If it is possible to acquire more than one VSP within a larger 3D surface acquisition, and before surface data are imaged with VSP-derived Green's functions, a number of issues are yet to be resolved. First, there is the question of how best to invert equation 4 for a robust estimate of scattering potential  $V$ . Then, the optimal weighted combination of  $V$  estimates (equation 7) should be found, and weights  $\phi$  and  $\varepsilon$  should be determined through experimentation.

## CONCLUSIONS

For accurate depth imaging, rather estimate imaging Green's functions from velocity models directly, Green's functions are obtained from measured subsurface scattering-potential  $V$ . Determination of  $V$  is shown to require more than one VSP for a given region. Then, with  $V$  computed for the region between source locations and VSP receiver locations, elastic variation and density variation estimated independently are used to perturb  $V$  to represent all surface / subsurface scattering potentials. Then,  $V$  all points in the image space are converted to Green's functions for use in depth imaging.

Because detailed maps of elastic variation and density variation are often impossible to obtain, perturbation of  $V$  for common-offset, common-azimuth gathers is proposed. Smooth variation in velocity is assumed, however, and density must be constant. Because these assumptions are consistent with conventional moveout analysis, perturbation of  $V$  from moveout analysis is developed.

## APPENDIX A

### APPROXIMATE $\Delta V$

Assume that, during surface acquisition, multiple VSPs (at least two) are live so that they record all offsets and all azimuths in the surface data are represented in the VSP data. Then, compute a table of common-offset-common-azimuth scattering potentials  $V$  according to equation 4. For surface imaging away from the VSP locations, then,  $V$  is perturbed according to equation 3. With the  $\nabla$  operators in the second term (equation 3)  $V$

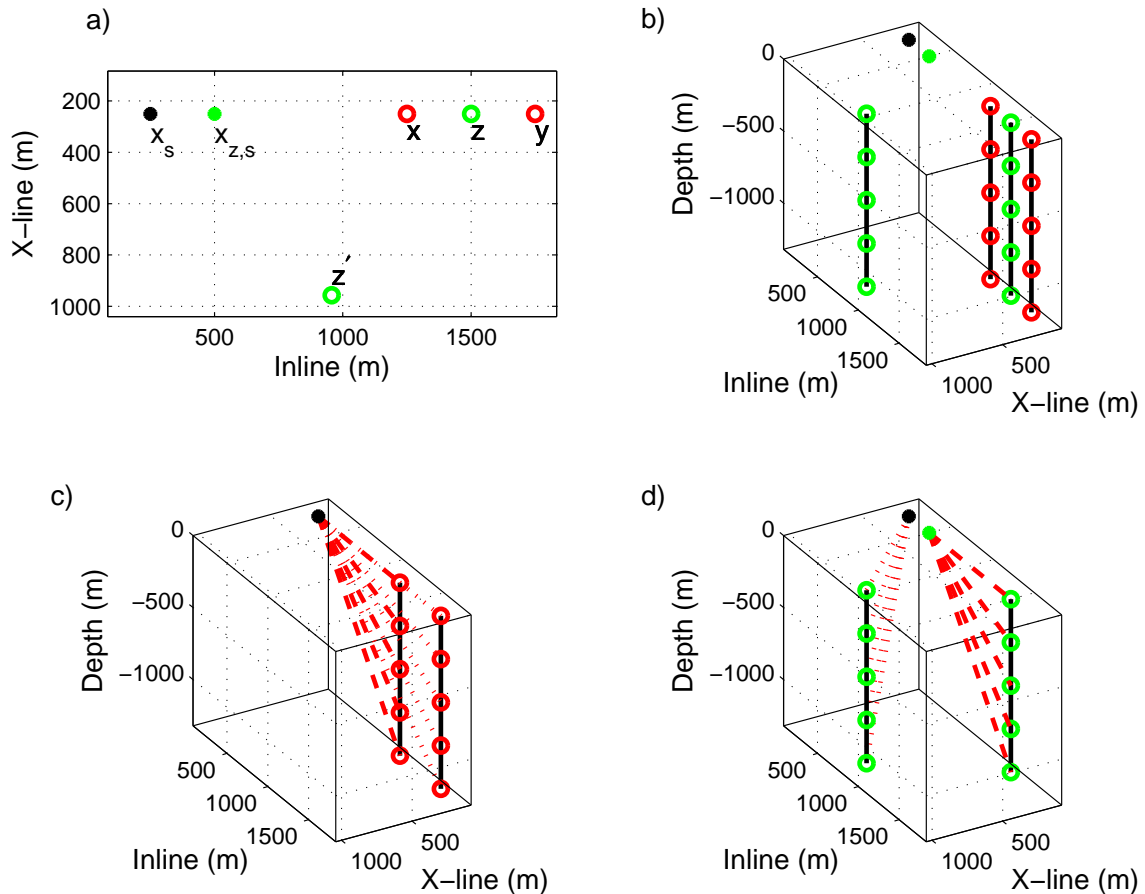


FIG. 1. Schematic of proposed VSP acquisition. a) Plan view. The black bullet indicates source location  $x_s$ , and red circles indicate VSP locations  $x$  and  $y$ . Locations where Green's functions are desired,  $z$  and  $z'$ , are represented by green circles. The green bullet represents virtual source  $x_{z,s}$  associated with  $z$ , and  $z'$  is an out-of-plane location associated with  $x_s$ . b) Same as a) but with a depth axis to indicate subsurface receiver locations. c) Following source initiation, wavefields (indicated by rays) are recorded in the VSP locations. d) Scattering potential  $V$  deduced from VSPs at  $x$  and  $y$  are used to compute Green's functions for  $z$  and  $z'$ .

is, perhaps, problematic numerically, however it simplifies significantly for constant  $\rho$  in that this term disappears. Further, if only P-wave data are acquired at the surface, S-wave velocity  $\beta$  is unknown, but this problem is resolvable if the ratio of  $\gamma = \alpha/\beta$  is assumed to be constant. Under these assumptions, the required derivatives of  $V$  in equation 10 simplify to

$$\frac{\partial}{\partial x} V = (1 + \gamma^{-1}) \frac{d\alpha}{dx} \frac{\partial}{\partial \alpha} V, \quad (\text{A-1})$$

where  $x \in \mathbb{R}^3$  is a general coordinate of space, and

$$\frac{\partial^2}{\partial x^2} V = (1 + \gamma^{-1}) \left( \frac{d\alpha}{dx} \right)^2 \frac{\partial^2}{\partial \alpha^2} V, \quad (\text{A-2})$$

and so on. Further, because moveout-derived  $\alpha$  estimates are smooth generally and

$$\frac{d\alpha}{dx} = \frac{\Delta\alpha}{\Delta x} + \epsilon, \quad (\text{A-3})$$

where  $\Delta\alpha = \alpha - \alpha_r$ . For  $\epsilon \ll 1$  (smooth variation of  $\alpha$ ), equation 10 becomes

$$\Delta V \approx (1 + \gamma^{-1}) \sum_{j=1}^{\infty} \frac{\Delta\alpha^j}{j!} \frac{\partial^j V}{\partial \alpha^j} \Big|_r. \quad (\text{A-4})$$

Equation A-4 is the scattering potential for constant  $\gamma$  and  $\rho$ , but with variable  $\alpha$ .

Under the acoustic assumption ( $\rho$  is still assumed to be constant)

$$\alpha = \sqrt{\kappa \rho}, \quad (\text{A-5})$$

and  $V$  (equation 3) reduces to

$$V \approx \omega^2 \left( \frac{1}{\kappa} - \frac{1}{\kappa_r} \right) = \frac{\omega^2}{\rho} \left( \frac{1}{\alpha^2} - \frac{1}{\alpha_r^2} \right). \quad (\text{A-6})$$

From equation A-6, we may estimate the required derivatives in equation A-4 according to

$$\frac{\partial^j V}{\partial \alpha^j} = (-1)^{(j+1)} \frac{(j+1)!}{\alpha^j} \left[ V + \left( \frac{\omega}{\alpha_r} \right)^2 \frac{1}{\rho} \right], 1 \leq j \leq \infty. \quad (\text{A-7})$$

Note that equation A-6 is written such that scattering potential  $V$  of the reference medium is explicit. Then, using equation A-7, and because in acoustic media

$$\gamma^{-1} = 0, \quad (\text{A-8})$$

$\Delta V_x$  is computed as

$$\Delta V = \left[ V + \left( \frac{\omega}{\alpha} \right)^2 \frac{1}{\rho} \right] \sum_{j=1}^{\infty} (-1)^{(j+1)} (j+1) \left( \frac{\Delta\alpha}{\alpha_r} \right)^j. \quad (\text{A-9})$$

Because, however,  $\Delta\alpha/\alpha \ll 1$  for smooth media, truncate equation A-9 according to

$$\Delta V = \left[ V + \left( \frac{\omega}{\alpha} \right)^2 \frac{1}{\rho} \right] \sum_{j=1}^N (-1)^{(j+1)} (j+1) \left( \frac{\Delta\alpha}{\alpha_r} \right)^j + \mathcal{O}^{N+1}, \quad (\text{A-10})$$

where  $\mathcal{O}^{N+1}$  are terms smaller than machine precision. For example, on a current workstation,  $N > 300$  underflow the memory within the range of values for  $\alpha$  in the earth.

## REFERENCES

- Brandesberg-Dahl, S., Hornby, B., and Xiao, X., 2007, Migration of surface seismic data with vsp green's functions: *The Leading Edge*, **26**, 778 – 780.
- Clayton, R. W., and Stolt, R. H., 1981, A Born-WKBJ inversion method for acoustic reflection data: *Geophysics*, **46**, 1559 – 1567.
- Fishmann, L., 2004, One-way wave equation modelling in two-way wave propagation problems: Vaxjo University Press, Sweden, Vaxjo, Sweden.
- Morse, P. M., and Feshbach, H., 1953, *Methods of theoretical physics*: McGraw Hill.